Kuramochi, H., Takahashi, K., Takita, T., & Umezawa, H. (1981) *J. Antibiot. 34*, 576–582.
Lane, M. J., Dabrowiak, J. C., & Vournakis, J. N. (1983) *Proc. Natl. Acad. Sci. U.S.A. 80*, 3260–3264.
Lane, M. J., Vournakis, J. N., & Dabrowiak, J. C. (1985) *Molecular Basis of Cancer* (Rein, R., & Liss, A. R., Eds.) Part B, p 145, Liss, New York.
Lown, J. W., & Sim, S. K. (1977) *Biochem. Biophys. Res. Commun. 77*, 1150–1157.
Lown, J. W., & Joshua, A. V. (1980) *Biochem. Pharmacol. 29*, 521–532.
Lown, J. W., & Joshua, A. V. (1982) *J. Chem. Soc., Chem. Commun.*, 1298–1300.
Lown, J. W., Hanstock, C. C., Bradley, R. D., & Scraba, D. G. (1984a) *Mol. Pharmacol. 25*, 178–184.
Lown, J. W., Plenkiewicz, J., Ong, C. W., Joshua, A. V., McGovren, J. P., & Hanka, L. J. (1984b) *Proceedings of the 9th International Union of Pharmacology Congress*, pp 265–269, Macmillan, London.
Maniatis, T., Fritsch, E. F., & Sambrook, J. (1982) *Molecular Cloning—A Laboratory Manual*, pp 458–472, Cold Spring Harbor Laboratory, Cold Spring Harbor, NY.
Maxam, A. M., & Gilbert, W. (1980) *Methods Enzymol. 65*, 499–560.
Moore, S. (1981) *Pancreatic DNase in the Enzymes* (Boyer, P. D., Ed.) Vol. 14, Part A, pp 281–296, Academic, New York.
Morgan, A. R., Evans, D. H., Lee, J. S., & Pulleyblank, D. E. (1979) *Nucleic Acids Res. 7*, 571–594.
Olsson, A., Moks, T., Uhlen, M., & Gaal, A. B. (1984) *J. Biochem. Biophys. Methods 10*, 83–90.
Povirk, L. F. (1983) in *Molecular Aspects of Anticancer Drug Action* (Neidle, S., & Waring, M. J., Eds.) pp 157–181, Macmillan, New York.
Sausville, E. A., Peisach, J., & Horwitz, S. B. (1978) *Biochemistry 17*, 2740–2746.
Schmitz, A., & Galas, D. J. (1979) *Nucleic Acids Res. 6*, 111–137.
Serwer, P., & Allen, J. L. (1984) *Biochemistry 23*, 922–927.
Spencer, C. F., Snyder, H. R., & Alaimo, R. J. (1975) *J. Heterocycl. Chem. 12*, 1319–1321.
Snyder, H. R., Spencer, C. F., & Freedman, R. (1977) *J. Pharm. Sci. 66*, 1204–1206.
Tapper, D. P., & Clayton, D. A. (1981) *Nucleic Acids Res. 9*, 6787–6794.
Van Dyke, M. W., Hertzberg, R. P., & Dervan, P. B. (1982) *Proc. Natl. Acad. Sci. U.S.A. 79*, 5470–5474.
Walden, P., & Kernbaum, A. (1890) *Chem. Ber. 23*, 1958–1961.
Walsh, C. (1979) *Enzymatic Reaction Mechanisms*, pp 464–500, Freeman, San Francisco.
Wells, R. D., Larson, J. E., Grant, R. C., Shortle, B. E., & Cantor, C. R. (1970) *J. Mol. Biol. 54*, 465–497.

Identification and Assignment of Base Pairs in Three Helical Stems of *Torulopsis utilis* Ribosomal 5S RNA and Its RNase T_1 and RNase T_2 Cleaved Fragments via 500-MHz Proton Homonuclear Overhauser Enhancements†

Shiow-meei Chen and Alan G. Marshall*
Departments of Biochemistry and Chemistry, The Ohio State University, Columbus, Ohio 43210
Received February 27, 1986; Revised Manuscript Received April 25, 1986

ABSTRACT: Imino proton resonances in the downfield region (10–14 ppm) of the 500-MHz ^{1}H NMR spectrum of *Torulopsis utilis* 5S RNA are identified (A·U, G·C, or G·U) and assigned to base pairs in helices I, IV, and V via analysis of homonuclear Overhauser enhancements (NOE) from intact *T. utilis* 5S RNA, its RNase T_1 and RNase T_2 digested fragments, and a second yeast (*Saccharomyces cerevisiae*) 5S RNA whose nucleotide sequence differs at only six residues from that of *T. utilis* 5S RNA. The near-identical chemical shifts and NOE behavior of most of the common peaks from these four RNAs strongly suggest that helices I, IV, and V retain the same conformation after RNase digestion and that both *T. utilis* and *S. cerevisiae* 5S RNAs share a common secondary and tertiary structure. Of the four G·U base pairs identified in the intact 5S RNA, two are assigned to the terminal stem (helix I) and the other two to helices IV and V. Seven of the nine base pairs of the terminal stem have been assigned. Our experimental demonstration of a G·U base pair in helix V supports the 5S RNA secondary structural model of Luehrsen and Fox [Luehrsen, K. R., & Fox, G. E. (1981) *Proc. Natl. Acad. Sci. U.S.A. 78*, 2150–2154]. Finally, the base-pair proton peak assigned to the terminal G·U in helix V of the RNase T_2 cleaved fragment is shifted downfield from that in the intact 5S RNA, suggesting that helices I and V may be coaxial in intact *T. utilis* 5S RNA.

5S RNA is found in the large subunit of all ribosomes except those of fungal and mammalian mitochondria (Thurlow et al., 1984) and is an essential component of ribosomal protein biosynthesis (Rohl & Nierhans, 1982; Brewer et al., 1983). Since its discovery (Rossett & Monier, 1963), 5S RNA has been studied intensively via genetic, enzymatic, chemical, and physical techniques in an effort to unravel its structure and the nature of its interactions with ribosomal proteins (Vandenberghe et al., 1985; Paleologue et al., 1985; Bohm et al., 1985; Kjems et al., 1985; Eigen et al., 1985; Curtiss &

†This work was supported by grants (to A.G.M.) from the U.S. Public Health Service (NIH 1 R01 GM-29274 and NIH 1 S10 RR-01458) and The Ohio State University.

0006-2960/86/0425-5117$01.50/0

Vournakis, 1984; Ohama et al., 1984; Delihas et al., 1984; Pieler et al., 1984; Nazar & Wildeman, 1983; Nazar et al., 1982).

Of the techniques reviewed in the above-cited references, the most direct and powerful for determining base-paired sequences is proton homonuclear Overhauser enhancements (NOE) (Johnston & Redfield, 1978), directed at the downfield (9–15 ppm) hydrogen-bond imino proton nuclear magnetic resonances of A·U, G·C, and G·U base pairs (Kearns et al., 1971; Kearns, 1977; Schimmel & Redfield, 1980; Reid, 1981). For example, NOE experiments have successfully identified virtually all of the secondary and tertiary base pairs in several tRNAs (Heerschap et al., 1982, 1983a,b; Hare & Reid, 1982a,b; Roy & Redfield, 1983) and several base-paired stems in 5S RNAs (Kime & Moore, 1983a,b; Kime et al., 1984; Li & Marshall, 1986; Chang & Marshall, 1986).

For 5S RNA, the major limitations of the NOE approach are (a) the secondary structure is not previously known from X-ray diffraction, as was the case for tRNAs, (b) 5S RNA contains 50% more nucleotides than tRNA, resulting in more frequent overlap of base-pair hydrogen-bond imino proton resonances, longer T_1, lower molar concentration for the same weight concentration, and greater peak widths, and (c) the tertiary folding pattern is not known.

Strategies available for RNA spectral assignment include ring current shift prediction (Hurd & Reid, 1979a,b; Shulman et al., 1973; Kime et al., 1984), isolation of enzymatic cleavage fragments (Boyle et al., 1980; Kime & Moore, 1983; Kime et al., 1984; Li & Marshall, 1986), spectral comparisons between RNAs of similar primary sequence (Rordorf et al., 1976; Hurd & Reid, 1979a; Chen, 1986), NOEs, and change in salt concentration or temperature to induce differential shifts in selected resonances Heerschap et al., 1982, 1983a,b; Kime & Moore, 1983; Li & Marshall, 1986; Chang & Marshall, 1986). The advantages offered by enzyme-cleaved fragments of 5S RNA are easy to apprehend: the RNA fragment has a lower molecular weight (therefore, shorter T_1 and narrower proton resonances) and contains fewer base pairs (and thus reduced overlap of resonances).

Yeast 5S RNAs have been found especially subject to cleavage at guanines 37 and 91 (see Figure 1) by the single-strand-specific ribonuclease T_1 (Vigne et al., 1973; Vigne & Jordan, 1977; Garrett & Olesen, 1982; Nishikawa & Takemura, 1974a; Nichols & Welder, 1979). After limited digestion under mild conditions, fragment B (residues 1–37) and fragment C (residues 92–121) can be purified via gel filtration under denaturing conditions (see supplementary material Figure 1; see paragraph at end of paper regarding supplementary material). When mixed in a 1:1 ratio, these two fragments pair together to comprise the "terminal" stem (I in Figure 1) (Luoma & Marshall, 1978; Luehrsen & Fox, 1981; Nishikawa & Takemura, 1974b), which is common to all of the three proposed 5S RNA secondary structure models (except for an extra segment pairing residues 13–16 with 111–108 in the cloverleaf model). Although the primary nucleotide sequences of *Torulopsis utilis* and *Saccharomyces cerevisiae* 5S RNA differ at six positions, most are proposed to occur in single-stranded regions; in particular, the terminal stems of both yeast 5S RNAs should be identical.

Yeast 5S RNA is reportedly very accessible to cleavage in the region containing residues 37–41 by a second single-strand-specific ribonuclease T_2 (Vigne et al., 1973; Vigne & Jordan, 1977; Garrett & Olesen, 1982). Digestion by RNase T_2 under very mild conditions yields a fragment containing residues 42–121, which should contain two major helical

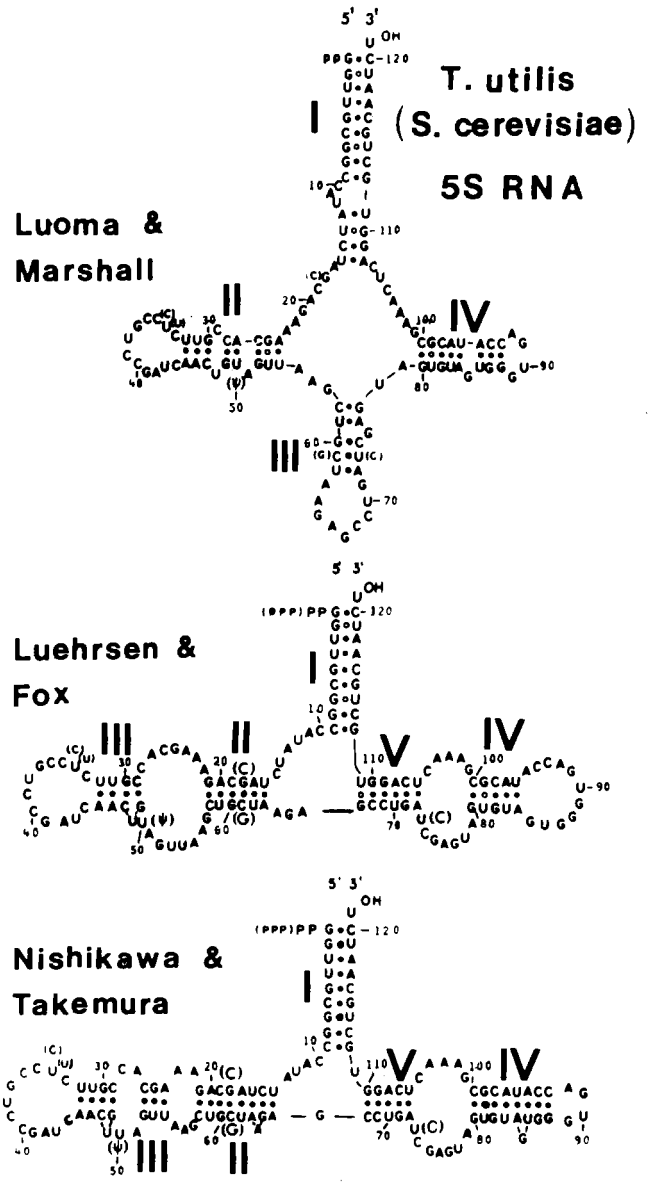

FIGURE 1: Three proposed 5S RNA secondary base-pairing schemes (Luoma & Marshall, 1978; Luehrsen & Fox, 1981; Nishikawa & Takemura, 1974b), adapted to the primary nucleotide sequences of *T. utilis* 5S RNA (Nishikawa & Takemura, 1974b) and *S. cerevisiae* 5S RNA (Masazumi, 1976). Bases shown in parentheses represent changes in proceeding from *T. utilis* to *S. cerevisiae*.

segments (IV and V in Figure 1). Helix IV has been shown to exist in prokaryotic (*Escherichia coli*) 5S RNA (Kime & Moore, 1983), but helix V has not yet been demonstrated experimentally.

The first proton NMR spectrum of a 5S RNA (which happened to be from yeast) was reported in 1972 (Wong et al., 1972). Because of the poor sensitivity of that 220-MHz instrument, a high RNA concentration (ca. 70 mg/mL) was needed to reveal the desired downfield base-pair hydrogen-bond imino proton resonances, and no individual peaks could be resolved. The next yeast 5S RNA study, this time at 360 MHz, appeared some 8 years later (Luoma et al., 1980). Even at 360 MHz, the high extent of peak overlap precluded assignment of individual resonances, and only the overall number of base pairs could be estimated. In this paper, we apply RNase T_1 and T_2 enzymatic cleavage and all four of the above-listed other proton NMR and NOE strategies to the identification and assignment of base-pair segments I, IV, and

V (see Figure 1) found in 5S RNAs from the two yeasts *T. utilis* and *S. cerevisiae*.

Materials and Methods

Isolation and Purification of Yeast 5S RNAs. Wild-type cells from both *Torulopsis utilis* and *Saccharomyces cerevisiae* were provided by the Fermentation Laboratory, Department of Microbiology, The Ohio State University. Extraction with 88% phenol and 1% sodium dodecyl sulfate (SDS) buffer at 8 °C and room temperature, respectively, followed by further purification via ion-exchange (DE-32) and gel filtration (Sephadex G-75) chromatography, yielded 5S RNA that was at least 90% pure as shown by 10% acrylamide gel electrophoresis in the presence of urea. Further details of the procedure may be found in Li et al. (1984).

T. utilis 5S RNA Fragments. T. utilis 5S RNA was treated with RNase T_1 to generate fragments by minor modification of Vigne et al. (1973). Intact 5S RNA was dissolved in 3 mM $MgCl_2$, 0.3 M NaCl, and 0.01 M tris(hydroxymethyl)-aminomethane hydrochloride (Tris-HCl), pH 7.5, at a concentration of 20 A_{260}/mL. RNase T_1 (Calbiochem) was added at 3.5 μL (=350 units) per milliliter of 5S RNA and incubated at 0 °C for 80 min. The reaction was stopped by addition of an equal volume of 5% SDS followed by phenol extraction twice. The fragments recovered from the aqueous layer were precipitated with 2.5 volumes of cold (−20 °C) ethanol.

RNase T_2 digestion of *T. utilis* 5S RNA was conducted according to Vigne et al. (1973) with little modification. 5S RNA was first dissolved to give a concentration of 20 A_{260}/mL in buffer containing 20 mM $MgCl_2$, 0.3 M NaCl, and 0.01 M Tris-HCl, pH 7.5. Two units of RNase T_2 (Sanka) per milliliter of RNA was added. After incubation at 0 °C for 50 h, the digestion was stopped, phenol-extracted, and precipitated as described for the RNase T_1 fragments.

Isolation and Purification of RNase-Cleaved Fragments of T. utilis 5S RNA. The RNase T_1 digested 5S RNA fragments were separated via Sephadex G-75 chromatography in 4 M urea, 50 mM NaCl, 1 mM ethylenediaminetetraacetic acid (EDTA), and 10 mM sodium cacodylate, pH 6.5, at room temperature. After the desired fractions were pooled, the samples were dialyzed for 4 h against 0.1 M NaCl–10 mM sodium cacodylate, pH 7.0, at 8 °C with one change of buffer to remove urea. The urea-free samples were then recovered by ethanol precipitation. RNase T_2 digested fragments were separated and recovered as described above except that the elution buffer for the G-75 column contained 8 M urea.

Gel Electrophoresis. 5S RNA and RNase-cleaved RNA fragments were tested for purity by gel electrophoresis in the presence of 8 M urea (Maxam & Gilbert, 1980). The gel was formed from 10% acrylamide, 0.5% bis(acrylamide), 0.08% TEMED, 8 M urea, and 0.05% ammonium persulfate in 100 mM Tris–borate, pH 8.3, and 2 mM EDTA buffer. Both intact 5S RNA and RNase-cleaved 5S RNA fragments were more than 90% pure as judged by their gel electrophoresis profiles (see supplementary material Figures 1 and 2).

Fragment Sequence Analysis. The primary nucleotide sequence of RNase T_1 digestion fragment C of *T. utilis* 5S RNA was confirmed to correspond to residues 92–121 (see Figure 1) in experiments kindly provided by B. A. Roe and R. Wilfon (Department of Chemistry, University of Oklahoma).

NMR Samples. T. utilis and *S. cerevisiae* 5S RNAs were dialyzed into 0.1 M NaCl, 10 mM EDTA, and 10 mM sodium cacodylate, pH 7.0, at 8 °C for 12 h with two changes of buffer and then against deionized water for 4 h with one change of water. After being freeze-dried, the RNA powders were dissolved in NMR buffer (100 mM NaCl, 1 mM EDTA, 5% D_2O, and 10 mM sodium cacodylate, pH 7.0) at an RNA concentration of 388 A_{260} units/0.4 mL of buffer (ca. 1 mM).

RNase-digested 5S RNA fragments were pooled and prepared as described above and then heated in a water bath at 65 °C for 5 min and cooled slowly down to room temperature in order to renature the RNA. The final RNA concentrations were 210 A_{260} units/0.4 mL of NMR buffer for RNase T_1 fragments B and C and 200 A_{260} units/0.4 mL of NMR buffer for RNase T_2 fragment A. Magnesium titrations were conducted by adding known aliquots of 0.25 M $MgCl_2$ solution to an RNA sample prior to NMR.

NMR Spectroscopy. All spectra were obtained with a Bruker AM-500 FT/NMR spectrometer, with phase-cycled quadrature detection (Chang & Marshall, 1986). Chemical shifts were measured relative to H_2O and referenced to DSS [3-(trimethylsilyl)-1-propanesulfonic acid] from an independent calibration. Downfield shifts are defined as positive.

Water suppression for both NMR and NOE difference spectra was achieved via either a modified Redfield 214-pulse sequence (Redfield et al., 1975) with the radio-frequency carrier centered at 15 ppm (i.e., 5100 Hz away from water resonance) or a 1331 hard-pulse sequence (Hore, 1983) with the carrier centered at the water resonance. An acquisition period of 147 ms and a relaxation delay of 0.5 s were typical. Further suppression for the 214 pulse was provided by alternate delay acquisition (Roth et al., 1980). With either excitation, the final spectrum gave a base line that required little or slight flattening.

NOE difference spectra were obtained according to Chang and Marshall (1986). Relatively low decoupler power (γB_1 = 15 Hz) was used for selective saturation (irradiation time < 0.5 s, to prevent extensive spin–diffusion) of the resonance of interest with off-resonance irradiation at 15 ppm. NOE difference spectra were apodized to give a line broadening of 5 Hz in order to enhance the signal-to-noise ratio. All spectra were obtained at 23 °C except where otherwise indicated.

Results and Discussion

Indentification of Base Pairs (A·U, G·C, G·U). The 500-MHz proton FT/NMR downfield spectra of 5S RNAs from *T. utilis* and *S. cerevisiae* are shown in Figure 2. The three main base-pair types may be identified by their characteristic homonuclear proton NOE difference spectra (Figures 3 and 4 for *T. utilis*), as discussed in detail elsewhere (Johnson & Redfield, 1978; Hare & Reid, 1982a,b; Li & Marshall, 1986; Chang & Marshall, 1986). For example, an A·U base pair may be identified by its NOE difference signal at ca. 7–8 ppm, corresponding to transfer of nuclear polarization from the A·U base-pair hydrogen-bond uracil N3 imino proton to the sharp resonance from the C2 proton of adenine in that pair, as seen in Figure 3B,C. In fact, the two sharp NOE's just below 7 ppm in Figure 3C establish that peak C includes two A·U pairs. In contrast, a G·C pair typically exhibits a broad NOE in the 7–9 ppm region, arising from polarization transfer from the G·C base-pair hydrogen-bond guanine N1 imino proton to the nearby amino protons of guanine and cytosine, which are broadened by relatively rapid exchange with H_2O (see Figure 3D for peak G). Finally, both hydrogen-bonded base-pair protons of a G·U "wobble" pair contribute NMR signals in the 10–12.5 ppm region, with very strong (20–40%) mutual NOE's (e.g., K and L in Figure 4B,C; K and P in Figure 4B,D; M and N in Figure 4E,F) due to the close proximity of the two hydrogen-bond protons in a G·U base pair. Because of their easily recognized NOE pattern, G·U pairs offer an attractive starting point for base-pair assignment (Chang & Marshall, 1986).

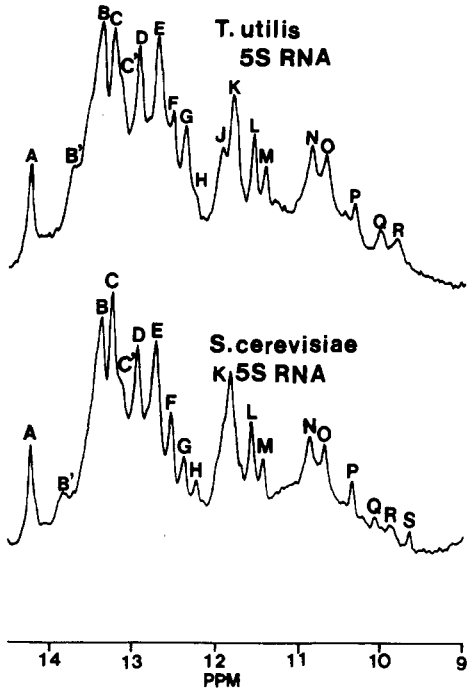

FIGURE 2: Proton 500-MHz FT/NMR spectra (downfield region) of *T. utilis* 5S RNA (top) and *S. cerevisiae* 5S RNA (bottom).

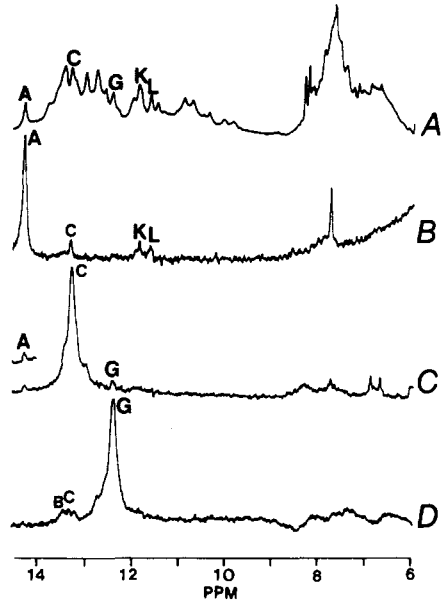

FIGURE 3: Proton 500-MHz FT/NMR spectrum of *T. utilis* 5S RNA (top) and NOE difference spectra (bottom) resulting from irradiation of peaks A, C, and G for 0.4 s at 0.2 mW.

Base-Pair Sequencing via NOE Connectivity. (A) T. utilis 5S RNA. The NOE difference spectra in Figures 3 and 4 reveal small (ca. 2–3%) NOE connections arising from transfer of nuclear polarization from an imino hydrogen-bond proton of one base pair to an imino hydrogen-bond proton of the base pair located immediately above or below it in a helical base-paired segment.

Consider first the three *T. utilis* G·U base pairs identified in Figure 4 as peaks K/L, K/P, and M/N. Irradiation of peak K produces strong mutual NOE's to peaks L and P (Figure 4B–D); thus, peak K contains resonances from two different G·U base pairs (K/L and K/P).

Irradiation of either peak K or peak P produces a weak NOE connection to peak B, which shows G·C NOE behavior (broad NOE in aromatic region, data not shown) and could

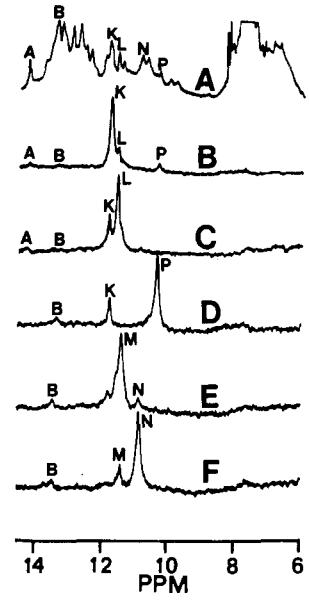

FIGURE 4: Proton NOE difference spectra resulting from irradiation of peaks K, L, P, M, and N of *T. utilis* 5S RNA. Format is as in Figure 5.

include up to four overlapped component base-pair protons. However, if peak B were to contain four base-pair protons, then irradiation of B could produce as many as eight NOE connectivities to nearest-neighbor base pairs, and we could not determine which of them corresponds to the B peak component that is adjacent to the G·U at K/P. [Irradiation of peak B (not shown) does give a weak NOE back to peak K.] Thus, we can infer that peaks K/P and B correspond to a G·U–G·C segment, but further sequencing is rendered inconclusive because of the multiplicity of peak B.

The next G·U (peaks M/N in Figure 4E,F) also shows weak NOE connectivity to the G·C resonances at peak B, corresponding to a second G·U–G·C segment. Unfortunately, inspection of the various proposed secondary structural models (Figure 1) reveals four possible G·U–G·C segments in the secondary structure alone, so that we cannot uniquely assign either of the above G·U–G·C segments to a particular location in the primary nucleotide sequence, based solely on NOE's of the intact 5S RNA.

Peaks K and L from the third G·U pair both show weak NOE connectivity to peak A (Figure 4B,C), which can be identified as an A·U pair from its chemical shift (14.26 ppm) and sharp NOE difference signal at 7.75 ppm (Figure 3B). As expected, irradiation of peak A gives weak NOE's back to peaks K and L. Thus, peaks K/L and A reveal a G·U adjacent to an A·U somewhere in the RNA structure. Proceeding further, peaks A and C exhibit weak mutual NOE's (Figure 3B,C). Irradiation at peak C reveals that it contains two A·U's (see preceding section), one of which is weakly NOE connected to peak G. Again, since peak C contains two A·U's, we cannot assume that peaks A–C–G form a consecutive base-pair sequence. At this stage, we can only assign the K/L–A–C sequence as a G·U–A·U–A·U segment. [The NOE experiment does not reveal the parity (A·U vs. U·A) of a given base pair.] Referring to Figure 1, we find only one possible G·U–A·U–A·U segment in any of the three proposed 5S RNA secondary structures. Therefore, assuming that the K/L–A–C peaks all arise from secondary (as opposed to tertiary) base pairs, we can tentatively assign the K/L–A–C segment as G_2·U_{119}–U_3·A_{118}–U_4·A_{117} in the terminal stem.

(B) S. cerevisiae 5S RNA. The primary sequence of *S. cerevisiae* 5S RNA differs from that of *T. utilis* 5S RNA in

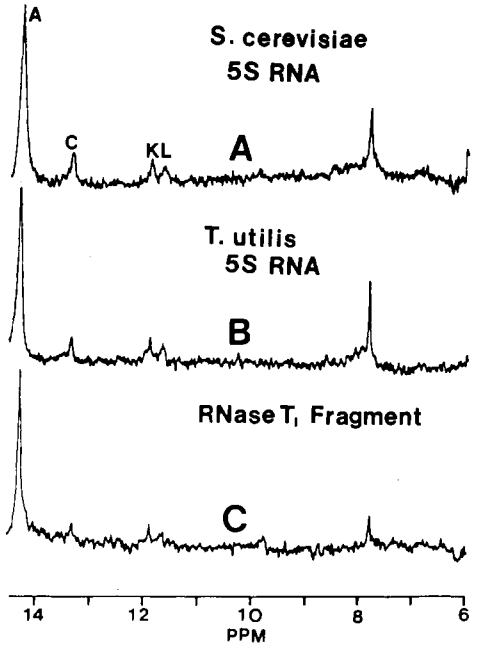

FIGURE 5: Proton NOE difference spectra resulting from irradiation of peak A of (A) *S. cerevisiae* 5S RNA, (B) *T. utilis* 5S RNA, and (C) RNase T_1 digested fragment of *T. utilis* 5S RNA.

only six nucleotide positions, most of which are predicted to fall in single-stranded segments (see Figure 1). If the two species have homologous secondary/tertiary structures, then we expect that at most two secondary base pairs should differ between these two yeast 5S RNAs. Figure 2 confirms that the downfield proton NMR spectra of the two 5S RNA species are indeed highly similar. Since the chemical shifts of RNA base-pair hydrogen-bond imino protons are known to be extremely sensitive to the type of nearest-neighbor base pair and to RNA conformation (as affected by salt, temperature, and/or denaturants), the near-identical spectra for the two yeast 5S RNAs offer strong evidence for near-identical secondary/tertiary structures in the two molecules.

A more direct test is provided by NOE experiments, which should reveal any changes in conformation or adjacent base pair type. Figure 5A,B shows that the NOE difference spectrum obtained via irradiation of peak A in either *T. utilis* or *S. cerevisiae* 5S RNA is almost identical, as are the NOE patterns from irradiation of peaks K, L, P, and M (compare Figure 4 and supplementary material Figure 3). These NOE results establish that the two yeast 5S RNAs have virtually identical secondary/tertiary structure at the base-pair locations corresponding to those resonances. Specifically, we can recognize the same base-pair segments previously sequenced from NOE's on *T. utilis* 5S RNA: G·U–G·C (peaks K/P–B); G·U–G·C (peaks M/N–B); G·U–A·U–A·U (peaks K/L–A–C). Finally, since no base-pair mutations between the two yeast 5S RNAs are predicted for the "terminal" stem, our previous assignment of peaks K/L–A–C as G_2·U_{119}–U_3·A_{118}–U_4·A_{117} is consistent with the identical NOE's for K/L–A–C in the two yeast species.

RNase T_1 Cleaved Fragments of T. utilis 5S RNA. RNase T_1 cleaved fragments of *T. utilis* were isolated in order to resolve the ambiguities in NOE connectivities involving multiple peaks and thereby afford a unique assignment of a particular base-pair sequence to a particular location in the RNA primary structure. Two of the fragments (see B and C in supplementary material Figure 1) from RNase T_1 digestion were combined in the hope of reconstituting just the terminal stem (helix I in Figure 1) of the secondary structure.

The downfield proton spectrum of intact *T. utilis* 5S RNA is presented in Figure 6A, together with its helix I reconstituted from RNase T_1 digestion fragments (Figure 6B) and an RNase T_2 cleaved fragment (Figure 6C). The first question is whether or not the secondary base pairing in the fragments is indeed the same as in the intact 5S RNA. Scrutiny of Figure 6 quickly reveals that most of the peaks in the spectrum of the RNase T_1 fragment correspond to peaks with the same chemical shift in the intact 5S RNA: e.g., peaks A, B, C, K (now split into K_1 and K_2), and P. Moreover, the NOE patterns for the fragment peaks A (Figure 5C) and L and P (supplementary material Figure 4C,D) are almost identical with those observed for the intact 5S RNA (Figure 5B and Figure 4C,D). Therefore, it is reasonable to infer that the conformation of the reconstituted helix I is very similar to that of the intact 5S RNA.

Peaks M and N are missing from the RNase T_1 fragment but remain in the RNase T_2 fragment, suggesting that the G·U–G·C segment assigned to peaks M/N–B is located in either helix IV or helix V (see Figure 1), as discussed below for the T_2 cleavage fragment.

Since peak K of the intact 5S RNA resolves into K_1 and K_2 in helix I reconstituted from RNase T_1 cleavage fragments, NOE experiments performed on helix I now show that the G·U–G·C segment of peaks K_1/L connects to peaks A and possibly B, whereas the G·U–G·C of peaks K_2/P connects only to B (see supplementary material Figure 4B,E). Thus, we can extend our G·U–A·U–A·U segment (peaks K/L–A–C) to G·C–G·U–A·U–A·U (peaks B–K_1/L–A–C), corresponding to G_1·C_{120}–G_2·U_{119}–U_3·A_{118}–U_4·A_{117}. Since peak K_2 represents a second G·U in the same terminal helix I, peaks K_2/P–B could represent either B_7·U_{114}–C_6·G_{115} or G_7·U_{114}–G_8·C_{113}. Temperature and salt dependence can be used to distinguish between these possibilities.

Heat-Induced Differential Melting of Base Pairs in Terminal Helical Stem. The 500-MHz proton FT/NMR spectra as a function of temperature for *T. utilis* 5S RNA and its reconstituted RNase T_1 fragments are shown in Figure 7 and supplementary material Figure 5, respectively. As the temperature increases, each of the base-pair hydrogen-bond imino proton resonances begins to lose intensity and broaden due to increased rate of chemical exchange with H_2O and eventually disappears when the base pair breaks. The temperature dependence of a particular base-pair proton resonance therefore reflects its thermal stability.

For example, peaks K_1/L and A begin to melt at 30 °C, whereas peaks K_2/P begin melting at about 39 °C. Such behavior is consistent with our prior assignment of K_1/L–A as G_2·U_{119}–U_3·A_{118}: the G·U–A·U segment should be the most thermally labile in helix I (Heus et al., 1983).

As least one component resonance from peak B persists up to 50 °C, whereas most of the others have melted at that temperature. It therefore seems highly likely that peaks K_2/P represent G_7·U_{114}, which is sandwiched in between two G·C base pairs above and below it in the terminal helix (see Figures 1 and 6).

Finally, peak B appears to contain two G·C resonances (from its relative intensity). One component is assigned as G_1·C_{120}, on the basis of the low melting temperature expected from end fraying of a terminal base pair (Boyle et al., 1980; Heus et al., 1983) and of its Mg^{2+}-dependent chemical shift (not shown) consistent with a tertiary or terminal base pair (Reid et al., 1979; Johnston & Redfield, 1981; Heerschap et al., 1983c). The remaining G·C resonance of peak B could be C_6·G_{115} or G_8·C_{113}, of which the former is expected to be

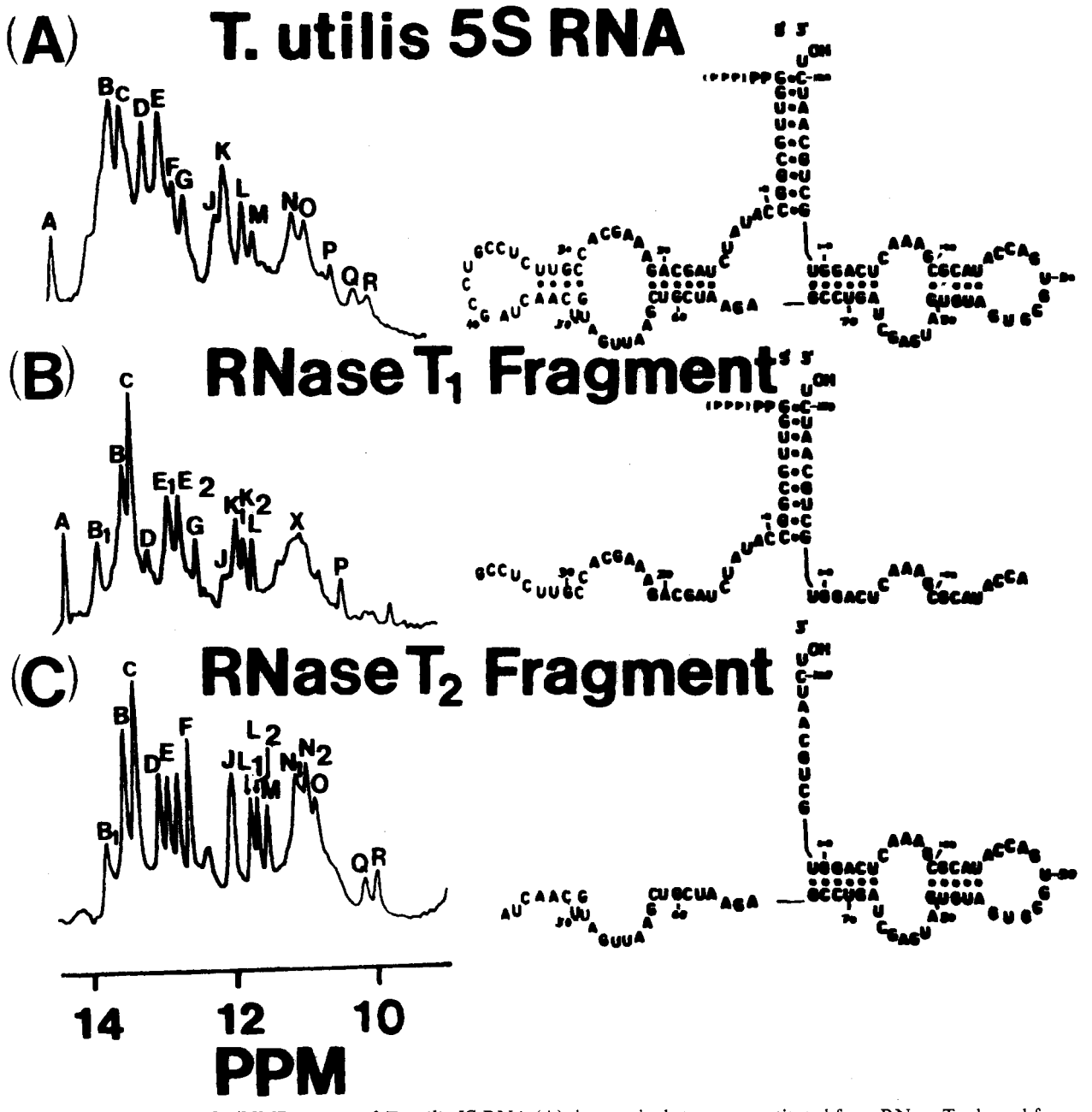

FIGURE 6: Proton 500-MHz FT/NMR spectra of *T. utilis* 5S RNA (A), its terminal stem, reconstituted from RNase T_1 cleaved fragments (B), and its RNase T_2 cleaved fragment (C). The corresponding base-pairing schemes shown at the right are based upon the Luehrsen and Fox model shown in Figure 1.

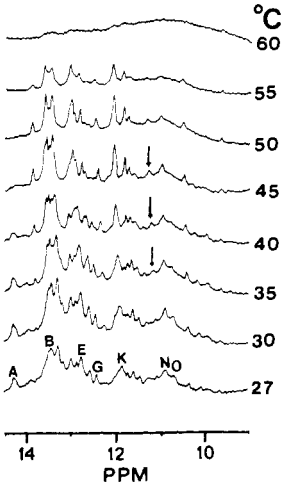

FIGURE 7: Proton 500-MHz FT/NMR spectra of *T. utilis* 5S RNA, at 27–60 °C.

more thermally stable because of its location near the center of the terminal helix.

Peak G (a G·C) and one of the A·U resonances of peak C also begin to melt (together) at about 30 °C in the reconstituted terminal helix fragment (supplementary material Figure 5). Since there is only one A·U–G·C segment in the terminal helix and since adjacent base pairs tend to melt at similar temperature, we tentatively assign peaks C and G as U_4·A_{117} and G_5·C_{116}.

At this stage, we have assigned seven of the nine base pairs of the terminal stem to nine resonances in the reconstituted terminal stem fragment: one resonance each for three G·C's and two A·U's and two resonances each for two G·U's. However, the reconstituted terminal helix fragment contains more than two additional resonances. For example, the hump (peak X) centered at 11 ppm in Figure 6B may arise from hydrogen bonds between the two free arms of fragments A and B (i.e., residues 12–37 and 121–92), because this signal

does not correspond to resonances observed in the intact 5S RNA. Moreover, the chemical shifts for N_3H of uridine and N_1H of guanosine dissolved separately in dry Me_2SO-d_6 resonate at 11.4 and 10.7 ppm, respectively (Hurd & Reid, 1979a,b). Thus, it is possible that some of the N_3H of U residues and/or N_1H of G residues are shielded from the solvent as a result of interactions between the two free arms of fragments A and B, with a sufficiently slow exchange rate with H_2O to render the signals NMR observable. Unpaired imino protons have been observed experimentally between 9 and 11 ppm (Hare & Reid, 1982b). Finally, most (ca. 70%) of the intensity from peak X in the reconstituted terminal helix melts at about 39 °C (supplementary material Figure 5), whereas peaks N and O in the same chemical shift region of intact 5S RNA persist up to 50 °C (Figure 7), again consistent with the assignment of peaks X as weak pairing between the two free arms of the reconstituted terminal helix fragment.

Although the primary nucleotide of RNase T_1 fragment C (supplementary material Figure 1) was confirmed to consist of residues 92–121 (see Figure 1) by direct RNA sequence analysis, fragment B from the RNase T_1 digest was not sequenced directly. However, our polyacrylamide gel electrophoresis pattern following 10-min RNase T_1 digestion (supplementary material Figure 1) is identical with that used by Vigne et al. (1973) to generate a fragment containing residues 1–37. Since proton NMR requires milligram amounts of RNA, we increased the RNase T_1 incubation time so that all of the 5S RNA would be digested, for maximum yield of the desired fragments. Although two small additional electrophoresis bands appear after 80-min digestion, the positions of bands B and C in 10% acrylamide gel are the same as for shorter digestion periods. Finally, other research groups (Nishikawa & Takemura, 1974a; Garrett & Olsen, 1982; Nichols & Welder, 1979) have independently reported similar RNase T_1 digestion results. Therefore, we are confident that the RNase T_1 digestion fragments do in fact correspond to segments 1–37 and 92–121.

RNase T_2 Cleaved Fragment of T. utilis 5S RNA. Fragment A (see supplementary material Figure 2) resulting from brief (5-min) RNase T_2 digestion of *T. utilis* 5S RNA has been shown via direct RNA sequencing to contain residues 42–121 (Vigne et al., 1973). In order to increase the yield of fragment A, we extended the digestion period to 50 h to give the polyacrylamide gel electrophoresis profile shown in supplementary material Figure 2. A shorter incubation period (20–30 min, not shown) yielded only the same fragments (A and D in supplementary material Figure 2) seen by Vigne et al. (1973). However, because the electrophoretic mobility of fragment A after 50-h digestion was the same as that after 30 min, we can be confident that fragment A in supplementary material Figure 2 is indeed the segment containing residues 42–121.

Comparison of the three spectra of Figure 6 shows that the reconstructed RNase T_1 cleavage fragments and the RNase T_2 fragment yield proton NMR spectra with complementary intensities in the base-pair hydrogen-bond imino proton resonance region (9–15 ppm). For example, peaks K/P assigned to a G·U in the terminal stem helix are absent from the RNase T_2 fragment. Also, the absence of interfering resonances in Figure 6C allows resolution of two resonances each at the positions labeled L and N in the intact 5S RNA spectrum. Each of the peaks of the RNase T_2 fragment was then irradiated in a one-dimensional NOE experiment.

Peaks M and N_2 of the RNase T_2 fragment form a G·U pair, on the basis of their chemical shifts (11.44 and 10.89 ppm) and strong (>10%) mutual NOE's (supplementary material Figure 6B,C). Both M and N_2 exhibit a weak NOE to peak B, which is itself a G·C pair on the basis of its chemical shift and NOE behavior (supplementary material Figure 6D). These results are almost identical with those seen for intact 5S RNA (Figure 4E,F and supplementary material Figure 3E), except that we were unable to detect the weak NOE's at M and N_2 upon irradiation of the G·C at peak B in the intact 5S RNA. Thus, the conformation of the RNase T_2 fragment appears to be the same (at least in this base-paired region) as that of the intact 5S RNA.

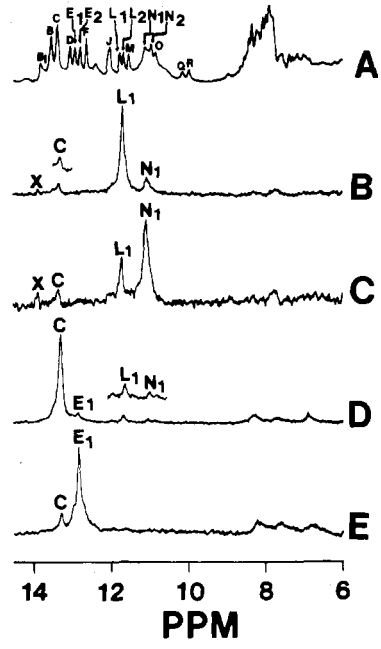

FIGURE 8: Proton NOE difference spectra resulting from irradiation of peaks L_1, N_1, C, and E_1 of the RNase T_2 fragment of *T. utilis* 5S RNA.

Peaks L_1 and N_1 of the RNase T_2 fragment form a fourth G·U pair on the basis of their chemical shifts and strong mutual NOE's (Figure 8B,C). Peaks L_1/N_1 give a weak NOE connectivity to peak C. Peak C probably represents two resonances, which show NOE connectivity to peaks L_1/N_1 and peak E_1 (Figure 8D,E). As has been noted previously for tRNAs and prokaryotic 5S RNA (Chang & Marshall, 1986), the fourth L_1/N_1 G·U pair shows NOE connectivity to only one (peak C) of its two neighboring base-pair hydrogen-bond imino protons. We cannot be sure of an L_1/N_1–C–E_1 base-pair sequence because of the presence of two resonance components at peak C.

Since we previously identified only three G·U pairs in the intact 5S RNA molecule (peaks K/L, K/P, and M/N), we cannot at this stage decide whether the fourth G·U pair (L_1/N_1) found in RNase fragment A arises from base pairing between the free arms of that fragment or is indeed present in intact 5S RNA but simply obscured by the many overlapping resonances in that region of the spectrum. We therefore repeated NOE irradiation of peaks L and N of the intact 5S RNA molecule, with a longer presaturation period (0.8 s rather than 0.4 s). The result (Figure 9) clearly shows an NOE connectivity between peak L and peaks N and C, as well as to peaks K, A, and B. Close scrutiny of Figure 4F suggests that irradiation of peak N gives a relatively broad NOE at peak M, which could include a contribution from peak L (only 0.16 ppm = 80 Hz away).

Heat-Induced Differential Melting and Shifts of Resonances from the RNase T_2 Fragment. Supplementary material

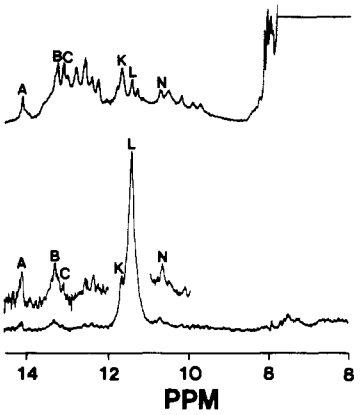

FIGURE 9: Proton NOE difference spectrum resulting from irradiation of peak L (0.8 s at 0.2 mW) of intact *T. utilis* 5S RNA.

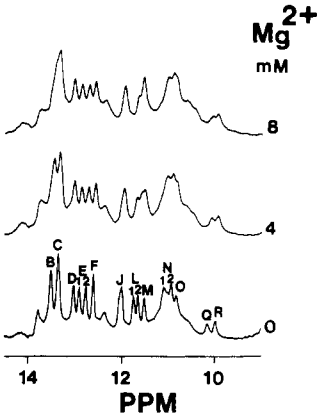

FIGURE 10: Proton 500-MHz FT/NMR spectra of the RNase T_2 fragment of *T. utilis* 5S RNA, as a function of $MgCl_2$ concentration.

Figure 7 shows a much larger downfield shift (from 11.0 to 11.3 ppm) for peak N_1 of the RNase T_2 fragment than for peak N_2 when the fragment is heated from 30 to 45 °C. This observation may account for the appearance of a new peak at 11.3 ppm on heating the intact 5S RNA (Figure 7). The differential shift for the RNase T_2 fragment confirms that peak N contains two resonances, as suggested by its high intensity in Figure 2.

Thus, we conclude that the four G·U base pairs observed in the two reassembled RNA fragments are in fact present in the intact 5S RNA. Since two have previously been identified in the terminal helix I stem, the other two must arise from helices IV and V. The presence of a G·U pair in helix V supports the secondary structure proposed by Luehrsen and Fox (1981) but does not rule out the equilibrium model proposed by DeWachter et al. (1984).

Figure 10 shows the NMR spectra resulting from titration of the RNase T_2 fragment with $MgCl_2$. Peaks B_1, B, L_1 (upfield shifts), and M (downfield shift) are Mg^{2+}-sensitive. If the observed resonances correspond to secondary (rather than tertiary) base pairs, then segment B–M/N_2 may be tentatively assigned as G_{80}·C_{100}–U_{81}·G_{99} on the basis that terminal or tertiary base pairs are more salt and temperature sensitive.

When we previously assigned L_1/N_1–C (G·U–G·C) and C–E_1 (G·C–G·C) segments, we suspected but could not demonstrate the L_1/N_1–C–E_1 (G·U–G·C–G·C) link. We now propose that L_1/N_1–C is G_{67}·U_{111}–C_{68}·G_{110}, on the basis of NOE's (one component of peak C looks like a G·C in Figure 8D) and of the Mg^{2+} and temperature sensitivity of peaks L_1 and N_1 that would be expected for a terminal G·U pair. The two possibilities for the C–E_1 segment in the secondary structure of the fragment containing residues 42–121 (see Figure 1) are C_{68}·G_{110}–C_{69}·G_{109} and G_{87}·C_{94}–C_{88}·C_{93}. Because both peaks C and E_1 are neither temperature nor Mg^{2+} sensitive (Figure 10 and supplementary material Figure 7) and because G_{88}·C_{93} would be a terminal base pair, we suggest that C_{68}·G_{110}–C_{69}·G_{109} is the most likely assignment.

A final base-pair connection (NOE difference spectra not shown) found in the RNase T_2 fragment is between peaks B_1 and J. Peak B_1 shows the sharp NOE at 7.4 ppm characteristic of an A·U base-pair imino proton, and peak J exhibits the broad aromatic NOE expected for a G·C base-pair imino proton. Their mutual NOE establishes an A·U–G·C segment. However, the small signals observed at peaks B and C on irradiation of peak B_1 are probably spillover of irradiation power, since we were unable to elicit an NOE signal at peak B_1 by irradiation of peak B (supplementary material Figure 6D) or peak C (Figure 8D). Also, peak J likely contains more than one resonance (on the basis of its relative intensity), thereby rendering weak NOE connectivities ambiguous. At best, we can only speculate from the Mg^{2+} broadening and low melting temperature of peak B_1 (Figure 10 and supplementary material Figure 7) that this segment is probably G_{82}·C_{98}–U_{83}·A_{97} and that the terminal A_{72}·U_{106} pair has already melted from the 23 °C spectrum (Heus et al., 1983).

Possible Coaxiality of Helix I and Helix V. The downfield shifts of peaks N_1 and L_1 of the RNase T_2 fragment compared to the corresponding N and L peaks in the intact 5S RNA (all other peaks retain the same chemical shifts in the RNase T_2 fragment as in the intact 5S RNA) could be explained by a disruption of coaxial stacking of helix I and helix V in the intact 5S RNA by removal of residues 1–41. On loss of its neighboring base pair from helix I, the terminal G_{67}·U_{111} base pair of helix V would be expected to shift downfield (Arter & Schmidt, 1976).

One-Sided NOE Connectivity for G·U Base Pair Resonances. For three of the four pairs of G·U base-pair hydrogen-bond protons observed in *T. utilis* 5S RNA and its enzyme-cleaved fragments, we observed NOE connectivity to only one of the nearest-neighbor base pairs. In each case, the Overhauser connection is seen to the base pair on the 3′-end (but not the 5′-end) of the G residue of the G·U pair, corroborating prior similar findings for a 16S RNA fragment (Heus et al., 1983) and for prokaryotic 5S RNA (Chang & Marshall, 1986).

SUMMARY

In conclusion, the present results most strongly support a Luehrson and Fox secondary structural model for yeast 5S RNA. In particular, we are able to identify base-paired segments located in helices I, IV, and V of that structure (helix V is unique to the Luehrson and Fox model). In the absence of specific evidence for tertiary base pairing and because tertiary base pairs tend to melt below proton NMR visibility at relatively low temperature, all of the spectral assignments in this paper have been to secondary base pairs only.

ACKNOWLEDGMENTS

We thank C. E. Cottrell for advice and assistance with NMR experiments and B. A. Roe and R. Wilfon for sequencing one of the RNase T_1 cleavage fragments of *T. utilis* 5S RNA. Finally, we also thank the Fermentation Lab of The Ohio State University for providing yeast cells.

SUPPLEMENTARY MATERIAL AVAILABLE

Two figures showing gel electrophoresis profile and five figures showing proton spectra of the 5S RNAs and their fragments used in this paper (8 pages). Ordering information

is given on any current masthead page.

References

Arter, D. B., & Schmidt, P. G. (1976) *Nucleic Acids Res. 3*, 1437–1447.

Bohm, S., Venyaminov, S. Y., Fabian, H., Fillmonov, V. V., & Welfle, H. (1985) *Eur. J. Biochem. 147*, 503–510.

Boyle, J., Robillard, G. T., & Kim, S.-H. (1980) *J. Mol. Biol. 139*, 601–625.

Brewer, L. A., Goolz, S., & Noller, H. F. (1983) *Biochemistry 22*, 4303–4309.

Chang, L.-H., & Marshall, A. G. (1986) *Biochemistry 25*, 3056–3063.

Chen, S.-M. (1986) Ph.D. Thesis, The Ohio State University.

Curtiss, W. C., & Vournakis, J. N. (1984) *J. Mol. Evol. 20*, 351–361.

Delihas, N., Anderson, J., & Singhal, R. P. (1984) *Prog. Nucleic Acid Res. Mol. Biol. 31*, 161–190.

DeWachter, R., Chen, M.-W., & Vandenberghe, A. (1984) *Eur. J. Biochem. 143*, 175–182.

Eigen, M., Linedmann, B., Winkler-Oswatitsch, R., & Clarke, C. H. (1985) *Proc. Natl. Acad. Sci. U.S.A. 82*, 2437–2441.

Garrett, R. A., & Olesen, S. O. (1982) *Biochemistry 21*, 4823–4830.

Hare, D. R., & Reid, B. R. (1982a) *Biochemistry 21*, 1835–1842.

Hare, D. R., & Reid, B. R. (1982b) *Biochemistry 21*, 5129–5131.

Heerschap, A., Haasnoot, C. A. G., & Hilbers, C. W. (1982) *Nucleic Acids Res. 10*, 6981–7000.

Heerschap, A., Haasnoot, C. A. G., & Hilbers, C. W. (1983a) *Nucleic Acids Res. 11*, 4483–4499.

Heerschap, A., Haasnoot, C. A. G., & Hilbers, C. W. (1983b) *Nucleic Acids Res. 11*, 4501–4520.

Heus, H. A., van Kimmenade, J. M. A., van Knippenberg, P. H., Haasnoot, C. A. G., DeBruin, S. H., & Hilbers, C. W. (1983) *J. Mol. Biol. 170*, 939–956.

Hore, J. (1983) *J. Magn. Reson. 55*, 283–300.

Hurd, R. E., & Reid, B. R. (1979a) *Biochemistry 18*, 4005–4011.

Hurd, R. E., & Reid, B. R. (1979b) *Biochemistry 18*, 4017–4024.

Johnston, P. D., & Redfield, A. G. (1978) *Nucleic Acids Res. 5*, 3913–3927.

Johnston, P. D., & Redfield, A. G. (1981) *Biochemistry 20*, 1147–1156.

Kearns, D. R. (1977) *Annu. Rev. Biophys. Bioeng. 6*, 477–523.

Kearns, D. R., Patel, D., & Shulman, R. G. (1971) *Nature (London) 229*, 338–339.

Kime, M. J., & Moore, P. B. (1983) *Biochemistry 22*, 2615–2622.

Kime, M. J., Gewirth, D. T., & Moore, P. B. (1984) *Biochemistry 23*, 3559–3568.

Kjems, J., Olesen, S. O., & Garrett, R. A. (1985) *Biochemistry 24*, 241–250.

Li, S.-J., & Marshall, A. G. (1986) *Biochemistry 25*, 3673–3682.

Li, S.-J., Chang, L.-H., Chen, S.-M., & Marshall, A. G. (1984) *Anal. Biochem. 138*, 465–471.

Leuhrsen, K. R., & Fox, G. E. (1981) *Proc. Natl. Acad. Sci. U.S.A. 78*, 2150–2154.

Luoma, G. A., & Marshall, A. G. (1978) *J. Mol. Biol. 125*, 95–105.

Luoma, G. A., Burns, P. D., Bruce, R. E., & Marshall, A. G. (1980) *Biochemistry 19*, 5456–5462.

Masazumi, M. (1976) *Nucleic Acids Res. 3*, s153–s156.

Maxam, A., & Gilbert, W. (1980) *Methods Enzymol. 65*, 499–560.

Nazar, R. N., & Wildeman, A. G. (1983) *Nucleic Acids Res. 11*, 3155–3168.

Nazar, R. N., Yaguchi, M., & Willick, G. E. (1982) *Can. J. Biochem. 60*, 490–496.

Nichols, J. L., & Welder, L. (1979) *Biochim. Biophys. Acta 561*, 445–451.

Nishikawa, K., & Takemura, S. (1974a) *J. Biochem. (Tokyo) 76*, 935–947.

Nishikawa, K., & Takemura, S. (1974b) *FEBS Lett. 40*, 106–109.

Ohama, T., Kumazaki, T., Hori, H., & Osawa, S. (1984) *Nucleic Acids Res. 12*, 351–361.

Paleologue, A., Reboud, A.-M., & Reboud, J.-P. (1985) *Eur. J. Biochem. 149*, 525–529.

Piler, T., Digweed, M., & Erdmann, V. A. (1984) in *Gene Expression* (Clark, B. F. C., & Petersen, H. U., Eds.) pp 353–376, Munksgaard, Copenhagen.

Redfield, A. G., Kunz, S. D., & Ralph, E. K. (1975) *J. Magn. Reson. 19*, 114–117.

Reid, B. R. (1981) *Annu. Rev. Biochem. 50*, 969–996.

Reid, B. R., McCollum, L., Ribeiro, N. S., Abbate, J., & Hurd, R. E. (1979) *Biochemistry 18*, 3996–4005.

Rohl, R., & Nierhans, K. H. (1982) *Proc. Natl. Acad. Sci. U.S.A. 79*, 729–733.

Rordorf, B. F., Kearns, D. R., Hawkins, E., & Chang, S. H. (1976) *Biopolymers 15*, 325–336.

Rossett, R., & Monier, R. (1963) *Biochim. Biophys. Acta 68*, 653–656.

Roth, K., Kimber, B. J., & Feeney, J. (1980) *J. Magn. Reson. 41*, 302–309.

Roy, S., & Redfield, A. G. (1983) *Biochemistry 22*, 1386–1390.

Schimmel, P. R., & Redfield, A. G. (1980) *Annu. Rev. Biophys. Bioeng. 9*, 191–221.

Shulman, R. G., Hilbers, C. W., Kearns, D. R., Reid, B. R., & Wong, Y. P. (1973) *J. Mol. Biol. 78*, 57–69.

Thurlow, D. L., Mason, T. L., & Zimmermann, R. A. (1984) *FEBS Lett. 173*, 277–282.

Vandenberghe, A., Wassink, A., Raemaekers, P., DeBaere, R., Huysmans, E., & DeWachter, R. (1985) *Eur. J. Biochem. 149*, 537–542.

Vigne, R., & Jordan, B. R. (1977) *J. Mol. Evol. 10*, 77–86.

Vigne, R., Jordan, B. R., & Monier, R. (1973) *J. Mol. Biol. 76*, 303–311.

Wong, Y. P., Kearns, D. R., Reid, B. R., & Shulman, R. G. (1972) *J. Mol. Biol. 72*, 741–749.